New Journal of Physics
The open access journal at the forefront of physics

Deutsche Physikalische Gesellschaft DPG
IOP Institute of Physics

Published in partnership with: Deutsche Physikalische Gesellschaft and the Institute of Physics

OPEN ACCESS

RECEIVED
29 August 2014

ACCEPTED FOR PUBLICATION
24 November 2014

PUBLISHED
9 January 2015

PAPER

Critical states embedded in the continuum

M Koirala[1], A Yamilov[1], A Basiri[2], Y Bromberg[3], H Cao[3] and T Kottos[2]

[1] Department of Physics, Missouri University of Science and Technology, Rolla, MO-65409, USA
[2] Department of Physics, Wesleyan University, Middletown, CT-06459, USA
[3] Department of Applied Physics, Yale University, New Haven CT-06520, USA

E-mail: yamilov@mst.edu

Keywords: localization, bound states in the continuum, optical waveguide array

Abstract

We introduce a class of critical states which are embedded in the continuum (CSC) of a one-dimensional optical waveguide array with one non-Hermitian defect. These states are on the verge of being fractal and have real propagation constants. They emerge at a phase transition which is driven by the imaginary refractive index of the defective waveguide and it is accompanied by a mode segregation which reveals analogies with the Dicke super-radiance. Below this point the states are extended while above it they evolve to exponentially localized modes. An addition of a background gain or loss can turn these localized states into bound states in the continuum.

1. Introduction

A widespread preconception in quantum mechanics is that a finite potential well can support stationary solutions that generally fall into one of the following two categories: (a) bound states that are square integrable and correspond to discrete eigenvalues that are below a well-defined continuum threshold; and (b) extended states that are not normalizable and are associated with energies that are distributed continuously above the continuum threshold [1]. This generic picture has further implications. For example, it was used by Mott [2] in order to establish the existence of sharp mobility edges between localized and extended wavefunctions in disordered systems. Specifically, it was argued that a degeneracy between a localized and an extended state would be fragile to any small perturbation which can convert the former into the latter. Nevertheless, von Neumann and Wigner succeeded in producing a counterintuitive example of a stationary solution which is square integrable and its energy lies above the continuum threshold [3]. These so-called 'bound states in the continuum' (BIC) can provide a pathway to confine various forms of waves such as light waves [4–7], acoustic waves, water waves [8], and quantum waves [9], as much as to manipulate nonlinear phenomena in photonic devices for applications in biosensing and impurity detection [10]. Interestingly, these ideas have also migrated to the nonlinear domain [11].

Although most of the studies on the formation of BIC states have been limited to Hermitian systems there are, nevertheless, some investigations that address the same question in the framework of non-Hermitian wave mechanics [12]. Along the same lines, the investigation of defect modes in the framework of $\mathcal{PT}$ -symmetric optics [13–15] has recently attracted some attention. On many occasions, however, the resulting BIC states are associated with very complex potentials which are experimentally challenging.

In this paper we introduce a previously unnoticed class of critical states which are embedded in the continuum (CSC). We demonstrate their existence using a simple setup consisting of N coupled optical waveguides with one non- Hermitian (with loss or gain) defective waveguide in the middle. Similarly to BIC they have real propagation constants; albeit their envelope resembles a fractal structure. Namely, their inverse participation number I_2 scales anomalously with the size of the system N as

$$\mathcal{I}_2 \equiv \frac{\sum_n |\phi_n|^4}{\left(\sum_n |\phi_n|^2\right)^2} \sim \frac{\log(N+1)}{(N+1)}. \quad (1)$$

Above ϕ_n is the wavefunction amplitude at the nth waveguide. The CSC emerges in the middle of the band spectrum when the imaginary index of refraction of the defective waveguide $\epsilon_0^{(I)}$ becomes $|\epsilon_0^{(I)}| = 2V$ where V is the coupling constant between nearby waveguides. Below this value all modes are extended while in the opposite limit the CSC becomes exponentially localized with an inverse localization length $\xi^{-1} = \ln\left[2V/(|\epsilon_0^{(I)}| - \sqrt{(\epsilon_0^{(I)})^2 - 4V^2})\right]$. The localization-delocalization transition is accompanied by a mode re-organization in the complex frequency plane which reveals many similarities with the Dicke super/sub-radiance transition [16]. We can turn these exponentially localized modes into BIC modes by adding a uniform loss (for gain defect) or gain (for lossy defect) in the array, thus realizing BIC states in a simple non-Hermitian setup.

2. Model

We consider a one-dimensional array of $N = 2M + 1$ weakly coupled single-mode optical waveguides. The light propagation along the z-axis is described by the standard coupled mode equation [17]

$$i\lambda\!\!\!^{-}\frac{\partial \psi_n(z)}{\partial z} + V\left(\psi_{n+1}(z) + \psi_{n-1}(z)\right) + \epsilon_n \psi_n(z) = 0 \quad (2)$$

where $n = -M, \cdots, M$ is the waveguide number, $\psi_n(z)$ is the amplitude of the optical field envelope at distance z in the nth waveguide, V is the coupling constant between nearby waveguides and $\lambda\!\!\!^{-} \equiv \lambda/2\pi$ where λ is the optical wavelength in vacuum. The refractive index ϵ_n satisfies the relation $\epsilon_n = \epsilon_0^{(R)} + i\epsilon_n^{(I)}\delta_{n,0}$ where we have assumed that a defect in the imaginary part of the dielectric constant is placed in the middle of the array at waveguide $n = 0$. Below, without loss of generality, we will set $\epsilon_0^{(R)} = 0$ for all waveguides. Our results apply for both gain $\epsilon_0^{(I)} < 0$ and lossy $\epsilon_0^{(I)} > 0$ defects.

Substitution in equation (2) of the form $\psi_n(z) = \phi_n^{(k)} \exp(-i\beta^{(k)} z/\lambda\!\!\!^{-})$, where the propagation constant $\beta^{(k)}$ can be complex, leads to the Floquet–Bloch (FB) [18] eigenvalue problem

$$\beta^{(k)}\phi_n^{(k)} = -V\left(\phi_{n+1}^{(k)} + \phi_{n-1}^{(k)}\right) - \epsilon_n \phi_n^{(k)}; \quad k = 1, \cdots, N. \quad (3)$$

We want to investigate the changes in the structure of the FB modes and the parametric evolution of $\beta^{(k)}$ as the imaginary part of the optical potential $\epsilon_0^{(I)}$ increases.

Before we begin the analysis of the model, we would like to comment on the possibility of realizing such a system in an experiment. Firstly, due to the Kramers–Kronig relations the real and imaginary parts of the dielectric constant are not independent of each other; nevertheless it is possible to have the same $\epsilon_0^{(R)}$ for the defective waveguide as well by compensating for the changes in the $\epsilon_0^{(R)}$ at $n = 0$ by adjusting, for example, the width of this waveguide. Secondly, optical losses can be incorporated experimentally by depositing a thin film of absorbing material on top of the waveguide [19], or by introducing scattering loss in the waveguides [20]. Optical amplification can be introduced by stimulated emission in gain material or parametric conversion in nonlinear material [21].

3. Threshold behavior

We begin by analyzing the parametric evolution of $\beta^{(k)}$'s as a function of the non-Hermiticity parameter $\epsilon_0^{(I)}$. We decompose the Hamiltonian H_{nm} of equation (3) into a Hermitian part $(H_0)_{nm} = -V\delta_{n,m+1} - V\delta_{n,m-1}$ and a non-Hermitian part $\Gamma_{nm} = -i\epsilon_n^{(I)}\delta_{n,0}\delta_{n,m}$ i.e. $H = H_0 + \Gamma$. For $\epsilon_0^{(I)} = 0$ the eigenvalues and eigenvectors of $H = H_0$ are $\beta^{(k)} = -2V\cos(k\pi/(N+1))$ and $\phi_n^{(k)} = \sqrt{2/(N+1)}\sin\left[k(n\pi/(N+1) + \pi/2)\right]$. In the limit $N \to \infty$ the spectrum is continuous, creating a band $\beta \in [-2V, 2V]$ that supports radiating states.

As $\epsilon_0^{(I)}$ increases from zero the propagation constants move into the complex plane. Using, for small values of $\epsilon_0^{(I)}$, first order perturbation theory we get that $\beta^{(k)} \approx \beta_0^{(k)} + \Gamma_{k,k}$ where $\Gamma_{k,k} \approx -i\epsilon_0^{(I)}/(N+1)$. When the matrix elements of the non-Hermitian part of H become comparable with the mean level spacing $\Delta = 2V/N$ of the eigenvalues of the Hermitian part H_0, the perturbation theory breaks down. This happens when $|\epsilon_{cr}^{(I)}|/(N+1) \sim \Delta$ which leads to the estimation $|\epsilon_{cr}^{(I)}| \sim 2V$. In the opposite limit of large $|\epsilon_0^{(I)}|$, H_0 can be treated as a perturbation to Γ. Due to its specific form, the non-Hermitian matrix Γ has only one nonzero eigenvalue and thus, in the large $|\epsilon_0^{(I)}|$ limit, there is only one complex propagation constant corresponding to

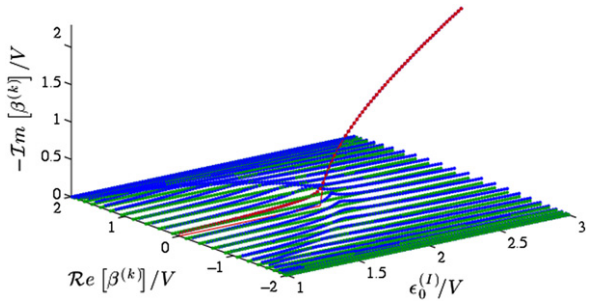

Figure 1. Parametric evolution of the propagation constants $\beta^{(k)}$ of an array of $N = 49$ coupled waveguides with one dissipative ($\epsilon_0^{(I)} > 0$) defect in the middle, as a function of $\epsilon_0^{(I)}$. The phase transition occurs at $\epsilon_0^{(I)} = \epsilon_{cr}^{(I)} \equiv +2V$ where the defect mode profile (shown as red dots) switches from non-exponential to exponential decay. The solid red line shows the asymptotic analytical result, equation (5). Similar behavior (not shown here) but with the β's in the upper complex plane can be observed for gain $\epsilon_0^{(I)} < 0$ where $\epsilon_{cr}^{(I)} = -2V$. The green lines indicate modes with real propagation constants which are solutions of the first equation (11). In the case of even number N they also acquire an imaginary part in the propagation constant, similar to the modes shown in blue.

$\mathcal{R}e\left[\beta_0^{(k\,=\,(N+1)/2)}\right] = 0$, while all other modes will have zero imaginary component (to first order). The above considerations allow us to conclude that for $|\epsilon_0^{(I)}| \gg 2V$ a segregation of propagation constants in the complex plane occurs: below this point all β's get an imaginary part which increases in magnitude as $\sim -\epsilon_0^{(I)}/N$ while after that only one of them accumulates almost the whole imaginary part $\sim -\epsilon_0^{(I)}$ (independent of N) and the remaining $N-1$ approaches back to the real axis as $\sim -(2V)^2/(N\epsilon_0^{(I)})$. This segregation of propagating constants is the analogue of quantum optics Dicke super-radiance transition [22] which was observed also in other frameworks [12, 23–25]. These predictions are confirmed by our numerical data (see figure 1).

4. Thermodynamic limit

In this section we investigate the structure of the FB modes of the system equation (3) in the thermodynamic limit ($N \to \infty$) as $\epsilon_0^{(I)}$ crosses the threshold $\epsilon_{cr}^{(I)}$. In the case of real defect, an infinitesimal value of it will lead to the creation of a localized mode (with a real-valued $\beta_{\rm def}$ outside of the interval $[-2V,\ 2V]$) [26]. We want to find out if the same scenario is applicable in the case of imaginary defect. To this end we introduce the ansatz:

$$\phi_n = \begin{cases} A^{(+)} \exp\left(-n\Lambda\right) & \text{for} \quad n \geqslant 0 \\ A^{(-)} \exp\left(n\Lambda\right) & \text{for} \quad n \leqslant 0. \end{cases} \tag{4}$$

The continuity requirement of the FB mode at $n = 0$ leads to $A^{(+)} = A^{(-)}$. Furthermore, substitute the above ansatz into equation (3) for $n = 0$ and $n = 1$ and after some straightforward algebra we get that

$$\beta_{\rm def} = -s\sqrt{4V^2 - \left(\epsilon_0^{(I)}\right)^2}; \quad \Lambda = -\ln\left(\frac{-\beta_{\rm def} - \mathrm{i}\epsilon_0^{(I)}}{2V}\right), \tag{5}$$

where $s \equiv \epsilon_0^{(I)}/|\epsilon_0^{(I)}|$ denotes the sign of the defect. From equation (5) we find that for $|\epsilon_0^{(I)}| < |\epsilon_{cr}^{(I)}| \equiv 2V$ the corresponding propagation constant is real while the decay rate is $\Lambda = -\mathrm{i}\arctan\left(\epsilon_0^{(I)}/\beta_{\rm def}\right)$ i.e. a simple phase. In other words the FB modes are extended. In the opposite limit of $|\epsilon_0^{(I)}| > |\epsilon_{cr}^{(I)}|$ the propagation constant becomes complex and the corresponding Λ takes the form

$$\Lambda = \ln\left(\frac{2\,V}{\left|\epsilon_0^{(I)}\right| - \sqrt{\left(\epsilon_0^{(I)}\right)^2 - 4V^2}}\right) + \mathrm{i}\,s\,\frac{\pi}{2} \tag{6}$$

The corresponding inverse localization length is then defined as $\xi^{-1} \equiv \mathcal{R}e\,(\Lambda)$ indicating the existence of exponential localization. Therefore we find that a non-Hermitian defect—in contrast to a Hermitian one (see for example [26])—induces a localization–delocalization transition at the phase transition points $\epsilon_{cr}^{(I)} = s \times 2V$. We emphasize again that this phase transition and the creation of a localized mode occur for both signs of the non-Hermitian defect and can be induced for both lossy ($\epsilon_0^{(I)} > 0$) and gain ($\epsilon_0^{(I)} < 0$) defect.

In figure 2 we report the FB defect mode of our system equation (3) for three cases (a) $0 < \epsilon_0 < 2V$, (b) $\epsilon_0 = 2V$ and (c) $\epsilon_0 > 2V$, and different system sizes. Note that, although in the latter case the mode is localized

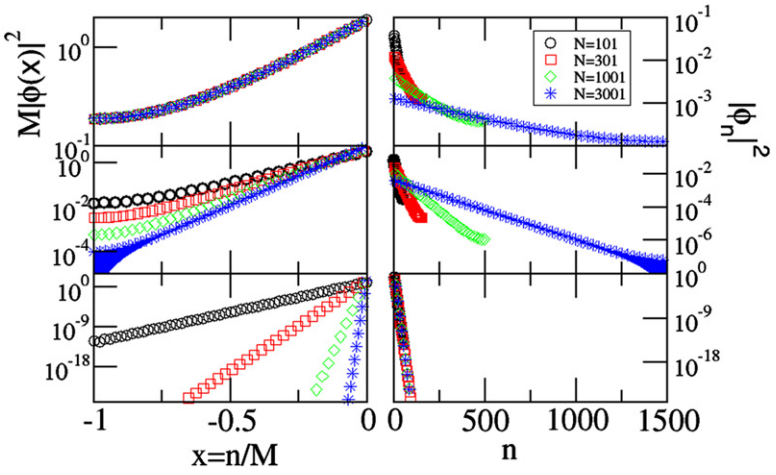

Figure 2. FB defect mode for various system sizes $N = 2M + 1$. Left panels report the left part ($n < 0$) of these modes (the right part $n > 0$ is the same) by employing the scaling $M\phi$ ($x = n/M$) while the right panels report the right part $n > 0$ of these modes without any scaling. In the former representation an extended state is invariant under increase of the size of the system while in the latter, the scale invariance is demonstrated for localized modes. Three defect values of $\epsilon_0^{(I)}$ have been used: (upper) $0 < \epsilon_0^{(I)} = 1.9\ V < 2V$ where the mode is delocalized; (middle) $\epsilon_0^{(I)} = 2V$ where the mode is critical; (lower) $\epsilon_0^{(I)} = 2.1\ V > 2V$ where the mode is exponentially localized.

in space, it is not qualified as a BIC since the corresponding propagation constant β_{def} (see equation (5)) is imaginary and therefore the mode is nonstationary. Adding, however, a uniform gain (for lossy defect) β_{def} or loss (for gain defect) $-\beta_{\mathrm{def}}$ to the array can turn this state into a BIC with zero imaginary propagation constant. The latter case is experimentally more tractable since adding a global loss will lead to a decay of all other modes while the localized defect mode would be stable with a constant amplitude.

5. Properties of the critical state

The existence of the delocalization-localization phase transition posses intriguing questions, one of which is the nature of the FB mode at the transition point associated with $\epsilon_{cr}^{(I)}$. In particular, it is known from the Anderson localization theory, that the eigenfunctions at the metal-to-insulator phase transition are multifractals i.e. they display strong fluctuations on all length scales [27–29]. Their structure is quantified by analyzing the dependence of their moments $\mathcal{I}_p$ with the system size N:

$$\mathcal{I}_p = \frac{\sum_n |\psi_n|^{2p}}{\left(\sum_n |\psi_n|^2\right)^2} \propto N^{-(p-1)D_p}. \tag{7}$$

Above, the multifractal dimensions $D_p \neq 0$ are different from the dimensionality of the embedded space d. Among all moments, the so-called inverse participation number (IPN) $\mathcal{I}_2$ plays the most prominent role. It can be shown that it is roughly equal to the inverse number of non-zero eigenfunction components, and therefore it is a widely accepted measure to characterize the extension of a state. We will concentrate our analysis on $\mathcal{I}_2$ of the FB mode at the phase transition point $\epsilon_{cr}^{(I)}$.

We assume that the eigenmodes of equation (3) take the form:

$$\phi_n^{(k)} = A^{(\mp)} e^{iq^{(k)}n} + B^{(\mp)} e^{-iq^{(k)}n} (n < 0/n > 0) \tag{8}$$

where $q^{(k)} = q_r^{(k)} + iq_i^{(k)}$, while the associated propagation constants are written in the form $\beta^{(k)} \equiv -2V \cos(q^{(k)}) = \beta_r^{(k)} + i\beta_i^{(k)}$. Imposing hard wall boundary conditions $\phi_{M+1} = \phi_{-M-1} = 0$ to the solutions equation (8) leads to:

$$B^{(\mp)} = -A^{(\mp)} e^{\mp 2iq(M+1)} \tag{9}$$

The requirement for continuity of the wavefunction at $n = 0$ leads us to the relation

$$A^{(+)} + B^{(+)} = A^{(-)} + B^{(-)} \tag{10}$$

Substitution of equations (9) and (10) back into equation (3) for $n = 0$, leads to the transcendental equations for q:

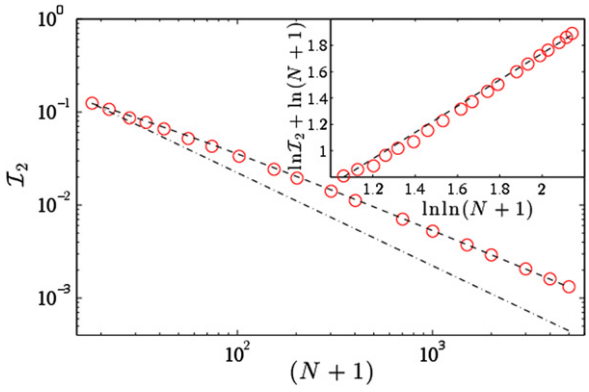

Figure 3. Scaling analysis of $\mathcal{I}_2$ (shown as symbols) of a CSC state versus the system size N. The dot-dashed line corresponds to N^{-1} dependence. The dashed line is the prediction of equation (1) which contains a logarithmic correction. In the inset we plot the same data in a different fashion i.e. $\ln \mathcal{I}_2 + \ln(N+1)$ versus $\ln\ln(N+1)$. The straight line with a unit slope confirms the existence of the logarithmic dependence as indicated by equation (1).

$$\sin[(M+1)q] = 0; \quad \text{or} \quad \cot[(M+1)q]\sin(q) = \mathrm{i}\frac{\epsilon_0^{(I)}}{2V}. \tag{11}$$

We are interested in the structure of the FB mode in the middle of the band corresponding to $\mathcal{R}e(\beta) = 0$. For simplicity of the calculations we assume below that $M+1$ is odd and also recall that the total size of the system is $N = 2M+1$. Imposing the condition $\mathcal{R}e(\beta) = 0$ in the second term of equation (11) we get that $q_r = -s\pi/2$ while the imaginary part q_i satisfies the equation

$$s\tanh\Big[(M+1)q_\mathrm{i}\Big]\cosh(q_\mathrm{i}) = \frac{\epsilon_0^{(I)}}{2V}. \tag{12}$$

We will look for a stationary solution at the phase transition point $\epsilon_0^{(I)} = s\,2V$ with $\beta_i \to 0$ (or equivalently $q_\mathrm{i} \to 0$) in $N \to \infty$ limit that also satisfies the condition $q_\mathrm{i} \times (M+1) \sim q_\mathrm{i} N \to \infty$. In equation (12) we now perform small q_i expansion in $\cosh(q_\mathrm{i}) \approx 1 + q_\mathrm{i}^2/2$ and large $(M+1)q_\mathrm{i}$ expansion in $\tanh[(M+1)q_\mathrm{i}] = \frac{\exp((M+1)q_\mathrm{i}) - \exp(-(M+1)q_\mathrm{i})}{\exp((M+1)q_\mathrm{i}) + \exp(-(M+1)q_\mathrm{i})} \approx 1 - 2\exp(-(N+1)q_\mathrm{i}) \approx 1 - q_\mathrm{i}^2/2$. In the large M-limit the solution of the last transcendental equation is

$$q_i \sim 2\frac{\ln(N+1)}{N+1}. \tag{13}$$

Substituting back in the expression for the propagation constant we get $\beta = -2V\cos(-s\pi/2 + \mathrm{i}q_\mathrm{i}) \approx -s\,2V\,\mathrm{i}q_\mathrm{i}$ which in the large N (M)-limit results in $\beta = 0$. Finally, substituting equations (9) and (13) back into equation (8) we get that

$$\phi_n \propto \exp\Big[\mathrm{i}\Big(-s\pi/2 + \mathrm{i}q_\mathrm{i}\Big)|n|\Big] = \frac{(-s\,\mathrm{i})^{|n|}}{(N+1)^{2|n|/(N+1)}}. \tag{14}$$

The FB state described by equation (14) is not exponentially localized neither it is extended. It rather falls into an exotic family of critical states and it can quantify better via the IPN $\mathcal{I}_2$. Using equation (7) for $p=2$ it is easy to show that the IPN of the FB mode of equation (14) is given by equation (1). Furthermore, this scaling relation is not consistent with the standard power law equation (7) characterizing self-similar (fractal) states. Rather we have an unusual situation of *a critical state that is on the verge of being fractal*. To our knowledge such anomalous scaling has been discussed only in the completely different context of Hermitian random matrix models [30] or modulated (graded) systems [31, 32] and were never found to be present in any physical system. Thus our simple setup constitutes the first paradigmatic system where these CSCs can be observed. In figure 3 we report the scaling of $\mathcal{I}_2$ versus the system size at the phase transition point $\epsilon_{cr}^{(I)} = 2V$ as found by solving equation (3) numerically. We see that the data follow nicely the prediction of equation (1).

We conclude this section by noting that for odd N considered above, some of the FB modes can have (due to symmetry) a nodal point at the center of the array where the non-Hermitian defect is placed, see green symbols in figure 1. Therefore they do not overlap with the defect and thus have real propagation constants. The latter are solutions of the first equation of (11). In the case of even N, all modes of the system are calculated by an equation similar to the second equation of (11) and thus they all have imaginary propagation constants. This is due to the fact that they have an appreciable component at the middle of the array where the non-Hermitian defect is

placed. The rest of the analysis associated with the CSC remains qualitatively the same. We also repeated our calculation for the periodic boundary conditions to confirm that the scaling properties for the critical state remain unchanged in the $N \to \infty$ limit.

6. Periodic perturbation

In this section we demonstrate that the critical nature of the defect state is not a consequence of the degenerate band-edge [33] being present in the case of the tight-binding system of equation (3). This can be achieved by introducing an on-site potential $\epsilon_n^{(R)} = \epsilon_0^{(R)}(-1)^n$ which removes the degeneracy at $\beta = 0$. Therefore, the new tight-binding equation is:

$$\beta^{(k)}\phi_n^{(k)} = -V\left(\phi_{n+1}^{(k)} + \phi_{n-1}^{(k)}\right) - \left(\epsilon_0^{(R)}(-1)^n + \mathrm{i}\epsilon_n^{(I)}\delta_{n0}\right)\phi_n^{(k)}; \tag{15}$$

We propose the following ansatz for odd/even (denoted by superscript o/e) waveguide numbers:

$$\begin{aligned}\phi_n^{(k)(o/e)} &= A^{(-)(o/e)}\mathrm{e}^{\mathrm{i}q^{(k)}n} + B^{(-)(o/e)}\mathrm{e}^{-\mathrm{i}q^{(k)}n}(n<0)\\ \phi_n^{(k)(o/e)} &= A^{(+)(o/e)}\mathrm{e}^{\mathrm{i}q^{(k)}n} + B^{(+)(o/e)}\mathrm{e}^{-\mathrm{i}q^{(k)}n}(n>0)\end{aligned} \tag{16}$$

In the absence of imaginary defects we get the following dispersion relation:

$$\beta^{(k)} = (-1)^b\sqrt{\left(\epsilon_0^{(R)}\right)^2 + 4V^2\cos^2 q^{(k)}}, \tag{17}$$

where b is the band index. $b = 1$ for $\mathcal{R}e[\beta] < 0$ and $b = 2$ for $\mathcal{R}e[\beta] > 0$. Therefore, the degenerate energy at zero is shifted into the positive or negative branch.

In the presence of a defect, and after taking into account the hard wall boundary conditions ($\phi_{M+1}^{(k)(o)} = \phi_{-M-1}^{(k)(o)} = 0$) and continuity at n = 0, we get two discrete equations for the complex propagation constant q:

$$\begin{aligned}&\sin[(M+1)q] = 0; \quad \text{or}\\ &\cot[(M+1)q]\sin(q) = \tfrac{\mathrm{i}\epsilon_0^{(I)}}{2V}\cdot\frac{\epsilon_0^{(R)} + (-1)^b\sqrt{\left(\epsilon_0^{(R)}\right)^2 + 4V^2\cos^2 q}}{2V\cos q}.\end{aligned} \tag{18}$$

The above equations are consistent with the results presented in the previous section at the limit $\epsilon_0^{(R)} \to 0$.

In the localized regime ($|\epsilon_0^{(I)}| > |\epsilon_{cr}^{(I)}|$), we get $\cot[(M+1)q] \approx \mathrm{i}$. By replacing this expression into the second term of equation (18), we derive the following cubic relation for $x \equiv \tan q$:

$$2\epsilon_0^{(R)}\epsilon_0^{(I)}x^3 + \left(\left(\epsilon_0^{(I)}\right)^2 - 4V^2\right)x^2 + 2\epsilon_0^{(R)}\epsilon_0^{(I)}x + \left(\epsilon_0^{(I)}\right)^2 = 0. \tag{19}$$

The above algebraic equation has three roots. Depending on the value of $\epsilon_0^{(I)}$ these roots can be either real or complex. In the former case (i.e. x, and therefore q, being real) the associated mode is extended, while in the latter one (i.e. x, and therefore q, being complex) the associated mode is localized. The transition between these types of modes occurs at $\epsilon_{cr}^{(I)}$ and is given as a solution of the following equation:

$$\left(\left(4V^2 - \epsilon_{cr}^{(I)}\right)^2\right)^3 = 8\left(\epsilon_0^{(R)}\right)^2\left(-2V^4 + 10V^2\left(\epsilon_{cr}^{(I)}\right)^2 + \left(\epsilon_{cr}^{(I)}\right)^4 + 2\left(\epsilon_{cr}^{(I)}\right)^2\left(\epsilon_0^{(R)}\right)^2\right). \tag{20}$$

Furthermore, it can readily be confirmed that, as expected, for $\epsilon_0^{(R)} \to 0$, $\epsilon_{cr}^{(I)}$ approaches 2.

The associated energy β_{cr} of the defect (localized) mode is found after substituting the expression for $\epsilon_{cr}^{(I)}$ from equation (20), into equation (18). This allows us to evaluate $q^{(cr)}$ which can then be substituted into equation (17) in order to get an expression for β_{cr}. The obtained dependence of $\mathcal{R}e[\beta_{cr}]$ on $\epsilon_0^{(R)}$ is shown in figure 4 by the red line. The values of $\mathcal{I}m[\beta_{cr}]$ are denoted by dots and numbers. We note that the real part of the propagation constant $\mathcal{R}e[\beta_{cr}]$ is insensitive to the sign of $\epsilon_0^{(I)}$.

Next, we investigate the scaling behavior of the defect mode at the transition point $\epsilon_{cr}^{(I)}$. Following the same argument as used in the previous section, we write $q^{(cr)}$ as $q_r^{(cr)} + \mathrm{i}q_\mathrm{i}$, where we assume that $(M+1)q_\mathrm{i} \to \infty$ and q_i is a small quantity. Substituting back to the transcendental equality of equation (18) and expanding each term up to first order in q_i we eventually get:

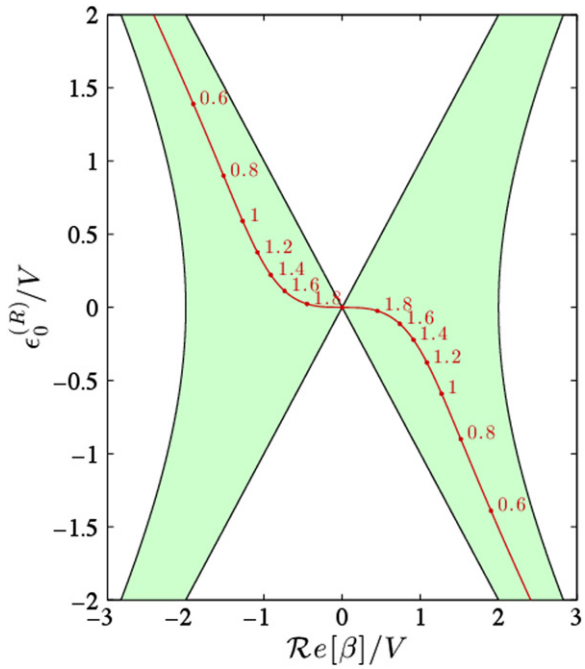

Figure 4. Band structure (green shadowed array) of the model equation (15) versus $\epsilon_0^{(R)}$. The red line indicates the trajectory of the defect eigenmode as $\epsilon_0^{(R)}$ increases. The red dots and the associated numbers are indicative values of the critical $|\epsilon_0^{(I)}|$ (for the specific $\epsilon_0^{(R)}$) above which a defect mode is created.

$$q_{\mathrm{i}} \sim \frac{\ln\,(N+1)}{N+1}. \tag{21}$$

Considering the fact that $\mathcal{I}_2 \sim q_{\mathrm{i}}$, it can be deduced that the second moment of the defect mode for the modified model scales anomalously as indicated in equation (1) of the main text. Hence, we conclude that the logarithmic scaling of IPR is not a consequence of degenerate band-edge in the Anderson model at $\beta = 0$.

7. Conclusions

In conclusion we have investigated the structure of non-Hermitian defect states as a function of the defect strength. We have found that these states experienced a phase transition from delocalization to localization as the imaginary part of the refractive index in the defect waveguide approaches a critical value. At the transition point the inverse participation number of this mode scales as $\ln\,(N)/N$ indicating a weak criticality. This phase transition is accompanied by a mode re-organization which reveals analogies with the Dicke super-radiance. The transition survives periodic pertubations in the refractive index in the waveguide array and the anomalous logarithmic behavior of the inverse participation ratio at the critical point is preserved. It will be interesting to investigate whether this behavior survives in higher dimensions and other types of configurations including disordered [34–36] and continuous [37, 38] models.

Acknowledgments

We thank A Ossipov and Y Fyodorov for useful discussions. This work was sponsored partly by grants NSF ECCS-1128571, DMR-1205223, ECCS-1128542 and DMR-1205307 and by an AFOSR MURI grant FA9550-14-1-0037.

References

[1] Peres A 1993 *Quantum Theory: Concepts and Methods* (Dordrecht: Kluwer)
[2] Mott N F 1967 *Adv. Phys.* **16** 49
[3] von Neumann J and Wigner E 1929 *Z. Phys.* **30** 465–67
[4] Plotnik Y, Peleg O, Dreisow F, Heinrich M, Nolte S, Szameit A and Segev M 2011 *Phys. Rev. Lett.* **107** 183901
[5] Weimann S, Xu Y, Keil R, Miroshnichenko A E, Nolte S, Sukhorukov A A, Szameit A and Kivshar Y S 2013 *Phys. Rev. Lett.* **111** 240403
[6] Corrielli G, Valle D G, Crespi A, Osellame R and Longhi S 2013 *Phys. Rev. Lett.* **111** 220403

[7] Hsu C W, Zhen B, Lee J, Chua S, Johnson S G, Joannopoulos J D and Soljai M 2013 *Nature* **499** 188–91
[8] Porter R and Evans D 2005 *Wave Motion* **43** 29–50
Linton C M and McIver P 2007 *Wave Motion* **45** 16–29
[9] Capasso F, Sirtori C, Faist J, Sivco D L, Chu S G and Cho A Y 1992 *Nature* **358** 565–67
[10] Marinica D C, Borisov A G and Shabanov S V 2008 *Phys. Rev. Lett.* **100** 183902
[11] Yagasaki K, Champneys A R and Malomed B A 2005 *Nonlinearity* **18** 2591–13
Gonzalez-Perez-Sandi S, Fujioka J and Malomed B A 2004 *Physica* D **197** 86–100
[12] Okolowicz J, Ploszajczak M and Rotter I 2003 *Phys. Rep.* **374** 271–83
[13] Zhou K, Guo Z, Wang J and Liu S 2010 *Opt. Lett.* **35** 2928–30
[14] Regensburger A, Miri M A, Bersch C, Nager J, Onishchukov G, Christodoulides D N and Peschel U 2013 *Phys. Rev. Lett.* **110** 223902
[15] Longhi S 2014 *Opt. Lett.* **39** 1697
Molina M I and Kivshar Y S 2014 Embedded states in the continuum for PT-symmetric systems *Stud. Appl. Math.* **133** 337–50
[16] Celardo G L, Giusteri G G and Borgonovi F 2014 Cooperative robustness to static disorder: superradiance and localization in a nanoscale ring to model light-harvesting systems found in nature *Phys. Rev.* B **90** 075113
[17] Christodoulides D N, Lederer F and Silberberg Y 2003 *Nature* **424** 817–23
[18] Russell P and St J 1986 *Appl. Phys.* B **39** 231–46
[19] Guo A, Salamo G J, Duchesne D, Morandotti R, Volatier-Ravat M, Aimez V, Siviloglou G A and Christodoulides D N 2009 *Phys. Rev. Lett.* **103** 093902
[20] Eichelkraut T, Heilmann R, Weimann S, Stutzer S, Dreisow F, Christodoulides D N, Nolte S and Szameit A 2013 *Nat. Commun.* **4** 2533
[21] Ruter C E, Makris K G, El-Ganainy R, Christodoulides D N, Segev M and Kip D 2010 *Nat. Phys.* **6** 192–95
[22] Dicke R H 1954 *Phys. Rev.* **93** 99–10
[23] Sokolov V V and Zelevinsky V G 1989 *Nucl. Phys.* A **504** 562–88
[24] Celardo G L, Borgonovi F, Merkli M, Tsifrinovich V I and Berman G P 2012 *J. Phys. Chem.* C **116** 22105–654
Monshouwer R, Abrahamsson M, Mourik F V and Grondelle R V 1997 *J. Phys. Chem.* B **101** 7241–48
[25] Keaveney J, Sargsyan A, Krohn U, Hughes I G, Sarkisyan D and Adams C S 2012 *Phys. Rev. Lett.* **108** 173601
Scully M O and Svidzinsky M M 2010 *Science* **328** 1239–41
[26] Economou E N 2006 *Green's Functions in Quantum Physics* (*Springer Series in Solid-State Sciences*) 3rd edn (Berlin: Springer)
[27] Mirlin A D 2000 *Phys. Rep.* **326** 259–382
Fyodorov Y V and Mirlin A D 1994 *Int. J. Mod. Phys.* **8** 3795
Fyodorov Y V and Mirlin A D 1995 *Phys. Rev.* B **51** 13403–9
[28] Falko V I and Efetov K B 1995 *Europhys. Lett.* **32** 627–32
Falko V I and Efetov K B 1995 *Phys. Rev.* B **52** 17413
[29] Wegner F 1980 *Z. Phys.* B **36** 209–14
Aoki H 1983 *J. Phys.* C **16** L205–08
Schreiber M and Grussbach H 1991 *Phys. Rev. Lett.* **67** 607–10
Parshin D A and Schober H R 1999 *Phys. Rev. Lett.* **83** 4590
Mildenberger A, Evers F and Mirlin A D 2002 *Phys. Rev.* B **66** 033109–14
[30] Ossipov A, Rushkin I and Cuevas E 2011 *J. Phys.: Condens. Matter* **23** 415601
[31] Zheng M, Goda M, Yakubo K and Yu K W 2008 *J. Phys. Soc. Japan* **77** 094601
[32] Yakubo K, Xiao J J and Yu K W 2007 *J. Phys.* **92** 012008
[33] Deych L I, Erementchouk M V, Lisyansky A A and Altshuler B L 2003 *Phys. Rev. Lett.* **91** 096601
[34] Parris P E 1989 *Phys. Rev. Lett.* **62** 1392
[35] Ziletti A, Borgonovi F, Celardo G L, Izrailev F M, Kaplan L and Zelevinsky V G 2012 *Phys. Rev.* B **85** 052201
[36] Basiri A, Bromberg Y, Yamilov A, Cao H and Kottos T 2014 *Phys. Rev.* A **90** 043815
[37] Joannopoulos J D, Johnson S G, Winn J N and Mead R D 2007 *Photonic Crystals: Molding the Flow of Light* (Princeton, NJ: Princeton University Press)
[38] Figotin A and Gorentsveig V 1998 *Phys. Rev.* B **58** 180